

# JOINT TEXTURE AND TOPOGRAPHY ESTIMATION FOR EXTENDED DEPTH OF FIELD IN BRIGHTFIELD MICROSCOPY

*François Aguet, Dimitri Van De Ville, and Michael Unser*

Biomedical Imaging Group  
Ecole Polytechnique Fédérale de Lausanne

## ABSTRACT

Brightfield microscopy often suffers from limited depth of field, which prevents thick specimens from being imaged entirely in-focus. By optically sectioning the specimen, the in-focus regions can be acquired over multiple images. Extended depth of field methods aim at combining the information from these images into a single in-focus image of the texture on the specimen's surface. The topography provided by these methods is limited to a map of the selected in-focus image for every pixel and is inherently discretized, which limits its use for quantitative evaluation. In this paper, we propose a joint texture and topography estimation, based on an image formation model for a thick specimen incorporating the point spread function. The problem is stated as a least-squares fitting where the texture and the topography are updated alternately. The method also acts as a deconvolution operation when the in-focus image has some blur left, or when the true in-focus position falls in-between two slices. The feasibility of the method is demonstrated with simulated and experimental results.

## 1. INTRODUCTION

The limited depth of field of conventional brightfield microscopes is an important shortcoming when the specimen's profile covers more than the system's depth of field. For such thick samples, which are often stained, the visible information is restricted to the texture that appears on the surface. Due to the limited depth of field, only parts of the sample appear in focus and sharp, while other regions remain out-of-focus and are blurred by the system's point spread function (PSF). A common solution is "optical sectioning"; i.e., a series of images is acquired by gradually changing the focus, which moves the specimen through the focal plane. Extended depth of field (EDF) algorithms facilitate the visualization and analysis of the specimen's texture by combining the in-focus information from multiple images into a single image that is entirely in-focus.

---

This work was supported by the Hasler foundation, as well as by the Swiss National Science Foundation under grant 200020-109415.

From this point on, we refer to the visible information on the specimen's surface as the *texture*, and to the surface's profile as the *topography*. Most EDF techniques concentrate on the recovery of the texture only. Nevertheless, accurate information on the specimen's topography could turn out as valuable additional information for the microscopist; e.g., for quantitative measurements such as surface area estimation of particular regions identified from the texture, or for 3-D visualization using "texture mapping".

Many EDF methods have been proposed in the literature; an overview can be found in [1, 2]. Almost every method boils down to three essential steps: (1) application of a high-pass filter slice-by-slice, (2) energy measurement in the local neighborhood around a pixel  $(i, j)$  in every slice, (3) selection of the slice with maximum energy as the in-focus position for the position  $(i, j)$ . A popular and computationally efficient approach is the variance method, which combines steps (1) and (2) by computing the variance in a local neighborhood. Another interesting class of methods are based on multi-resolution decompositions [3] such as the wavelet transform [4, 5]. By applying the wavelet transform to every slice, one automatically performs high-pass filtering at different resolutions. This approach avoids the choice of a fixed local neighborhood. The selection of the in-focus slice is performed in the wavelet domain too; i.e., at every resolution level. In the end, these EDF methods mainly yield the texture, while the topography is only a map of the selected in-focus slice for every pixel. By construction, such a topography contains unrealistic "staircase" effects.

In this paper, we propose a joint texture and topography estimation, which is based on a physically-inspired image formation model. Specifically, we express the signal as the convolution between the texture mapped onto a thin surface layer that follows the topography, and the PSF of the system (cf. Sect. 2). In Sect. 3, we present our reconstruction algorithm that minimizes the quadratic error between the model and the measurements by alternate optimization of the texture and the topography. Compared to standard EDF techniques, the topography is not limited to discretized values anymore since it can change in a continuous way to maximally match the measurements. Furthermore, the estimation of the texture also acts as a deconvolution operation, in the case when a resid-

ual blur remains at the in-focus position, or when the true in-focus position falls in-between two slices. Compared to classical deconvolution, the texture estimation is better conditioned since the whole image stack contributes to its estimation. In Sect. 4, we discuss several useful PSF models and propose an empirical Gaussian PSF that can be useful for many practical cases. Finally, the proposed algorithm is demonstrated in Sect. 5 and experimental results are shown.

## 2. IMAGE FORMATION MODEL FOR THICK SPECIMENS

We propose to model the sample  $o(x, y, z)$  as a 3-D surface, described by its topography  $p(x, y)$ , onto which the texture  $f(x, y)$  is mapped. Mathematically, we write

$$o(x, y, z) = f(x, y)\delta(z - p(x, y)), \quad (1)$$

where the Dirac distribution represents the thin surface.

The image formation and acquisition process is modeled as the convolution between the object and the microscope's 3-D PSF,  $h(x, y, z)$ , followed by sampling to obtain the stack of images:

$$\tilde{s}(i, j, k) = \sum_{u, v \in \mathcal{S}_2} f(u, v)h(i - u, j - v, k - p(u, v)), \quad (2)$$

where  $\mathcal{S}_2$  is the 2-D support of the texture.

## 3. EXTENDED DEPTH OF FIELD

We propose a least-squares approach to jointly estimate the topography and the texture; i.e., we want to minimize the error function

$$\epsilon(f, p) = \sum_{i, j, k \in \mathcal{S}_3} \underbrace{\left( s(i, j, k) - \tilde{s}(i, j, k) \right)}_{e(i, j, k)}^2, \quad (3)$$

where  $\mathcal{S}_3$  is the 3-D support of the measured image stack  $s$ . For this purpose, we apply a two-step optimization method that alternately updates the texture and the topography, as illustrated in Fig. 1. We denote the texture and the topography at the  $\tau$ -th iteration as  $f^{(\tau)}$  and  $p^{(\tau)}$ , respectively.

### 3.1. Texture estimation

Given the initial or previous estimation of the topography, we estimate the texture by minimizing the error function (3) with respect to  $f$ :

$$f^{(\tau+1)} = \arg \min_f \epsilon(f, p^{(\tau)}). \quad (4)$$

This minimization is achieved by performing a steepest descent on  $\epsilon$  with respect to the texture  $f(m, n)$ . The partial derivatives  $\partial\epsilon/\partial f(m, n)$ , easily obtained by applying the

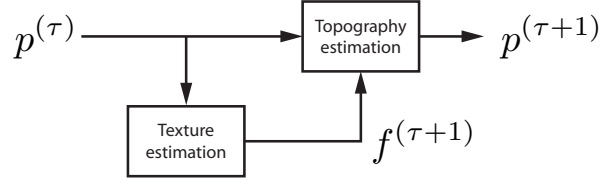


**Fig. 1.** Schematic representation of an iteration from the two-step optimization method.

chain rule, are given by

$$\begin{aligned} \frac{\partial\epsilon}{\partial f(m, n)} &= -2 \sum_{i, j, k \in \mathcal{S}_3} e(i, j, k)h(i - m, j - n, k - p^{(\tau)}(m, n)) \\ &= -2(e * h^T)(m, n, p^{(\tau)}(m, n)), \end{aligned}$$

where  $\cdot^T$  stands for the spatial transpose; i.e.,  $h^T(i, j, k) = h(-i, -j, -k)$ .

The gradient descent update step then consists of

$$f_{\text{update}}(m, n) = f(m, n) - \alpha \frac{\partial\epsilon}{\partial f(m, n)}, \quad (5)$$

where the factor  $\alpha > 0$  controls the strength of the update; its optimal value is obtained by performing a line search. Starting from  $f^{(\tau)}$ , several subiterations (5) are performed to finally obtain a new estimate of the texture  $f^{(\tau+1)}$ .

### 3.2. Topography estimation

Next, the topography can be updated using the latest texture estimate  $f^{(\tau+1)}$ . Similarly, we minimize the error function with respect to the topography:

$$p^{(\tau+1)} = \arg \min_p \epsilon(f^{(\tau+1)}, p). \quad (6)$$

The partial derivatives  $\partial\epsilon/\partial p(m, n)$  can be also be obtained using the chain rule as

$$\begin{aligned} \frac{\partial\epsilon}{\partial p(m, n)} &= 2f(m, n) \sum_{i, j, k \in \mathcal{S}_3} e(i, j, k)h_z(i - m, j - n, k - p(m, n)) \\ &= 2f(m, n)(e * h_z^T)(m, n, p(m, n)), \end{aligned}$$

where  $h_z$  corresponds to the partial derivative of the PSF with respect to  $z$ . Notice that the signal model  $\tilde{s}(i, j, k)$  inside the error term  $e(i, j, k)$  depends on the texture  $f^{(\tau+1)}$ .

Then, the gradient descent update step for the topography is

$$p_{\text{update}}(m, n) = p(m, n) - \alpha \frac{\partial\epsilon}{\partial p(m, n)}. \quad (7)$$

The subiterations are started from  $p^{(\tau)}$  and result in  $p^{(\tau+1)}$ .

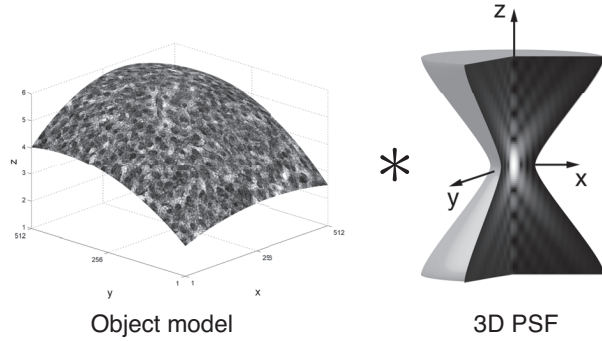


**Fig. 2.** Simulated acquisitions can be generated using the image formation model, i.e., by convolving a texture mapped surface with a 3-D PSF.

### 3.3. Some remarks

The algorithm requires an initial estimation of the topography. In our experiments, a simple initialization of the topography at a constant level worked well in all cases.

It should be noted that a limited number of subiterations for the steepest descent optimization are satisfactory. Indeed, the main importance is to improve the estimation of the texture (respectively, topography) after which the topography (respectively, texture) needs an update again anyway.

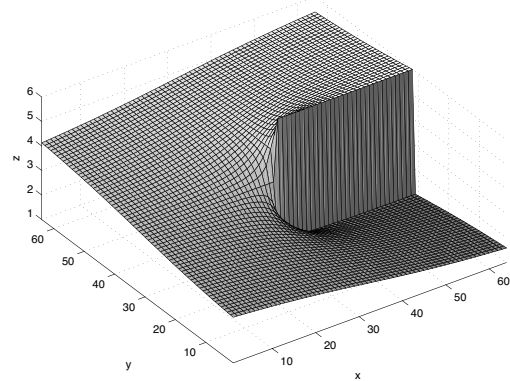
After each full iteration, the average update of the topography seemed to be an appropriate stopping criterion for the algorithm.

Interestingly, the current method can also be interpreted within the context of maximum-likelihood; in particular, the expectation-maximization (EM) algorithm. The expression of the likelihood can be obtained after adding a noise component to the signal model of (2). For additive white Gaussian noise, maximizing the likelihood is then identical to the minimization of (3). For the solution by the EM algorithm, the texture represents the quantity to be estimated while the topography corresponds to the hidden state. In the E-step, the texture is updated given the current hidden state. In the M-step, the hidden state is updated for the new texture.

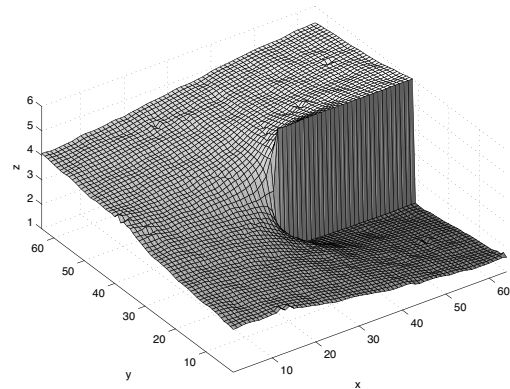
The concept can also be made more sophisticated by adding prior constraints on the topography and/or the texture, and considering an augmented regularized least squares (or MAP) criterion.

## 4. THEORETICAL PSF MODELS

The algorithm presented above is independent of the type of PSF model used. If required, it is therefore possible to use a highly accurate theoretical model that takes into account spatial non-stationarities and aberrations, such as the scalar model proposed by Gibson and Lanni [6]. Since models such as this one are usually formulated for a single wavelength, they must be integrated over the spectrum of the light source



(a)



(b)

**Fig. 3.** Result of the estimation on a simulated data set. (a) The topography used to generate a stack of images. (b) The topography recovered by our two-step optimization method. Discontinuities in the topography are well handled by the algorithm.

used. In modern brightfield microscopes, the light source is well balanced over the visible spectrum, which means that the PSF needs to be uniformly integrated over the interval of visible wavelengths. The result of this integration is essentially a smoothing effect; in fact the  $xy$ -sections of a white-light PSF closely resemble Gaussians. Since a Gaussian PSF model is computationally much more efficient than its more complex counterparts (at each iteration of the topography estimation, the PSF needs to be recomputed for every point), it is therefore advantageous to fit a Gaussian model to the real PSF's parameters and to use the former for computations. A good approximation can be obtained with a model of the following

form:

$$h(x, y, z) = \frac{1}{2\pi(c + |z|)^2} \exp\left(-\frac{(x^2 + y^2)}{2(c + |z|)^2}\right), \quad (8)$$

where  $c$  is a small constant. The simulations in the remaining sections of the paper were performed using this model.

Here it is important to mention that brightfield microscopes use Köhler illumination, which is designed to uniformly illuminate the sample, independently of the position of the focus. In order to take this into account, the PSF needs to be normalized such that the energy within each  $xy$ -section is identical.

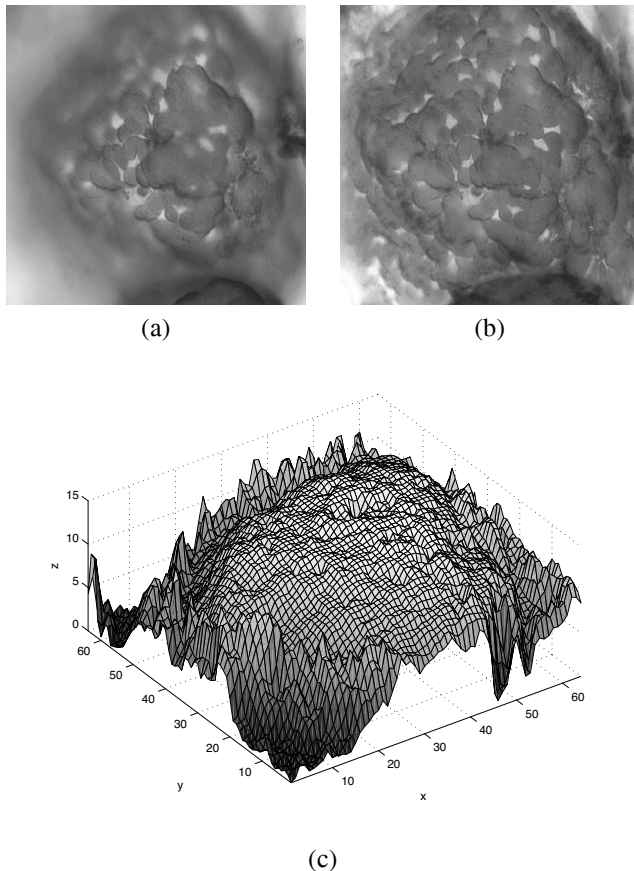


**Fig. 4.** Result of the joint texture and topography estimation on a biological specimen. (a) An optical section in which the focused and blurred regions are clearly visible. (b) The fused EDF image. (c) The estimated topography of the specimen.

## 5. RESULTS

To validate our algorithm, we generated simulated acquisitions using the object and image formation model; i.e. by applying the non-stationary convolution of (2) (see Fig. 2). This provided us with a ground truth for both the texture and the topography in order to assess the quality of the estimation.

An example is given in Fig. 3; a set of 6 optical sections was generated and used to estimate the topography, which was initially set to a constant value of 3. The result after convergence closely matches the ground truth, and the discontinuity is remarkably well preserved.

Finally, we tested our approach on a set of acquisitions of a biological specimen (see Fig. 4). We estimated the texture and topography from 15 optical sections of a segment of mouse intestine. The results clearly reveal the heap-like structure of the sample. The random behavior at the border of the topography is explained by the absence of any in-focus information for that region in our acquisitions.

## 6. CONCLUSION

We have presented a new approach for extended depth of field, where both the texture and the topography of the specimen are estimated. By applying this joint optimization to a stack of optical sections of a specimen, we have shown that the topography can be accurately recovered, without the discretization artifacts present in existing methods. We demonstrated the validity of the approach on simulated data sets that were generated with a known topography, and obtained promising results on a set of experimental acquisitions.

## 7. REFERENCES

- [1] A. G. Valdecasas, D. Marshall, J. M. Becerra, and J. J. Terrero, "On the extended depth of focus algorithms for bright field microscopy," *Micron*, vol. 32, pp. 559–569, 2001.
- [2] A. G. Valdecasas, D. Marshall, and J. M. Becerra, "Extended depth-of-focus algorithms in brightfield microscopy," *European Microscopy and Analysis*, vol. 79, pp. 15–17, September 2002.
- [3] P. J. Burt and R. J. Kolczynski, "Enhanced image capture through fusion," in *Fourth International Conference on Computer Vision*, 1993, pp. 173–182.
- [4] H. Li, B. S. Manjunath, and S. K. Mitra, "Multisensor image fusion using the wavelet transform," *Graphical Models and Image Processing*, vol. 57, no. 3, pp. 235–245, 1995.
- [5] B. Forster, D. Van De Ville, J. Berent, D. Sage, and M. Unser, "Complex wavelets for extended depth-of-field: A new method for the fusion of multichannel microscopy images," *Microscopy Research and Technique*, vol. 65, no. 1-2, pp. 33–42, 2004.
- [6] S. F. Gibson and F. Lanni, "Experimental test of an analytical model of aberration in an oil-immersion objective lens used in three-dimensional light microscopy," *Journal of the Optical Society of America A*, vol. 8, no. 10, pp. 1601–1613, 1991.